The Effect of Renal Failure on ^{18}F-FDG Uptake: A Theoretic Assessment

Eric Laffon[1–3], Anne-Laure Cazeau[1], Antoine Monet[1], Henri de Clermont[1], Philippe Fernandez[1], Roger Marthan[2,3], and Dominique Ducassou[1]

[1]CHU de Bordeaux, Service de Médecine Nucléaire, F-33600 Pessac, France; [2]Université Bordeaux 2, Laboratoire de Physiologie Cellulaire Respiratoire, F-33076 Bordeaux, France; and [3]INSERM U885, F-33076 Bordeaux, France

This work addresses the issue of using ^{18}F-FDG PET in patients with renal failure. **Methods:** A model analysis has been developed to compare tissue ^{18}F-FDG uptake in a patient who has normal renal function with uptake in a theoretic limiting case that assumes tracer plasma decay is tracer physical decay and is trapped irreversibly. **Results:** This comparison has allowed us to propose, in the limiting case, that the usually injected activity be lowered by a factor of 3. We also proposed that the PET static acquisition be obtained at about 160 min after tracer injection. These 2 proposals were aimed at obtaining a similar patient radiation dose and similar tissue ^{18}F-FDG uptake. **Conclusion:** In patients with arbitrary renal failure (i.e., between the 2 extremes of normal function and the theoretic limiting case), we propose that the injected activity be lowered (without exceeding a factor of 3) and that the acquisition be started between 45 and 160 min after tracer injection, depending on the severity of renal failure. Furthermore, the model also shows that the more severe the renal failure is, the more overestimated is the standardized uptake value, unless the renal failure indirectly impairs tissue sensitivity to insulin and hence glucose metabolism.

Key Words: ^{18}F-FDG PET radiation dose; renal failure; ^{18}F-FDG kinetic modeling

$\mathbf{A}$n ^{18}F-FDG PET examination begins with the intravenous injection of the tracer. Then, from blood, the tracer enters tissue cells, where it is phosphorylated and hence trapped. Conversely, the tracer can be dephosphorylated and therefore can go back to the blood while being simultaneously cleared from the blood by the kidneys. For simplicity, the ^{18}F-FDG blood time–activity curve can be assumed to exponentially decrease within a time period $T_{1/2}$. The value of this constant is critical since it is required to manage the acquisition timing (1,2) and to assess the tracer residence time ($\tau = 1.44$ $T_{1/2}$), which is involved in the patient radiation dose (3–5).

To the best of our knowledge, the issue of how to use ^{18}F-FDG PET in patients with renal failure has not yet been considered, except when intravenous CT contrast material is to be applied (6). The aim of this work was to establish a model describing tissue ^{18}F-FDG uptake in a theoretic limiting case that has allowed us to propose landmark injected activities and acquisition timings for use in clinical practice to reduce the radiation dose to the patient and medical staff.

MATERIALS AND METHODS

The limiting case is defined by theoretic conditions that lead, after an arbitrary ^{18}F-FDG injected activity, to the highest possible patient radiation dose and the longest possible time to peak tracer activity in the tissue. The first condition (highest possible dose) is fulfilled by assuming that the tracer plasma decay is the tracer physical decay (no biologic decay). The second condition (longest possible time to peak) is fulfilled with the first condition and by assuming that the tracer is trapped irreversibly.

In patients with normal renal function, a 2-compartment model (the blood pool is counted as 1 compartment) has been proposed to quantify the ^{18}F-FDG uptake rate in tissues, assuming the tracer is trapped irreversibly (1). At the steady state, the rate of trapped tracer change per tissue volume unit dC_T/dt is

$$dC_T/dt = KC_p(t) - \lambda C_T(t), \qquad \text{Eq. 1}$$

where K is the uptake rate constant, λ is the ^{18}F physical decay constant ($\lambda = \text{Log}2/110 \text{ min}^{-1}$), and $C_p(t)$ is the tracer concentration in the plasma at any time t. For simplicity, let us assume that $C_p(t)$ decays monoexponentially:

$$C_p(t) = C_p(t = 0)e^{-\alpha t}, \qquad \text{Eq. 2}$$

with $\alpha = (\text{Log}2)/T_{1/2}$. In patients with normal renal function, $T_{1/2}$ involves both the physical and the biologic decay of the tracer. Furthermore, $C_p(t = 0)$ is usually assessed by the ratio of the injected activity to the patient's weight, assuming that the patient's weight is proportional to the patient's volume ($C_p(t = 0) \approx A_{inj}/W$) (7). The solution of Equation 1 is

$$C_T(t) = Ke^{-\lambda t} \int_0^t Cp(\tau)e^{\lambda \tau}d\tau. \qquad \text{Eq. 3}$$

Therefore, the equation of the time–activity curve of trapped ^{18}F-FDG per tissue volume unit is

$$\lambda C_T(t) = \lambda K C_p(t=0)[(e^{-\lambda t} - e^{-\alpha t})/(\alpha - \lambda)]. \qquad \text{Eq. 4}$$

Furthermore, let us note that dividing Equation 4 by $\lambda C_p(t)$ yields a ratio R, which reflects the tumor-to-background ratio.

In the limiting case, when only the physical decay of the tracer occurs, that is, $T_{1/2} = 110$ min ($\alpha = \lambda$), the equation of the time–activity curve of trapped ^{18}F-FDG per tissue volume unit becomes

$$\lambda C_T(t) = \lambda K C_p(t=0)te^{-\lambda t}. \qquad \text{Eq. 5}$$

Furthermore, dividing Equation 5 by $\lambda C_p(t)$ yields a ratio R that is quite simple:

$$R = \lambda C_T(t)/(\lambda C_p(t)) = Kt. \qquad \text{Eq. 6}$$

RESULTS

Figure 1 shows the ^{18}F-FDG blood time–activity curves for $T_{1/2} = 110$ and 37 min, that is, in the limiting case and in patients without renal failure, respectively. The value of 37 min has been derived from $\alpha_3 = 0.0125 + 0.0063$ min^{-1} by Hunter et al., when the tracer physical decay is considered (8).

Figure 2 shows theoretic ^{18}F-FDG tissue time–activity curves from Equation 4 ($T_{1/2} = 37$ min) and Equation 5 ($T_{1/2} = 110$ min). The value of K has been arbitrarily set to 0.05 min^{-1} (9). The maximal tracer activity in the tissue occurs at about $t = 85$ and 160 min, for $T_{1/2} = 37$ and 110 min, respectively. At $t = 160$ min, the value of $C_T(t)$ for $T_{1/2} = 110$ min is 2.3 times greater than that at $t = 45$ min for $T_{1/2} = 37$ min. At the peak times, the value of $C_T(t)$ for $T_{1/2} = 110$ min is 1.9 times greater than that for $T_{1/2} = 37$ min, respectively. At $t = 60$ min after ^{18}F-FDG injection, the value of $C_T(t)$ for $T_{1/2} = 110$ min is 1.4 times greater than that for $T_{1/2} = 37$ min. When a triexponential input function is used (patients with normal renal function), the tracer activity peak is near that obtained with a monoexponential input function (<5 min difference).

The patient radiation dose depends on $T_{1/2}$ by way of the residence time; consequently, for the same amount of injected activity the factor of increase is about 3 ($\approx$110/37) in the limiting case, compared with patients with normal renal function.

Figure 3 shows the ratio R versus the time delay between injection and acquisition for $T_{1/2} = 37$ and 110 min: R is the ratio of the curves in Figure 2 to those in Figure 1. The values of R for $T_{1/2} = 37$ min in the 45- to 60-min range are
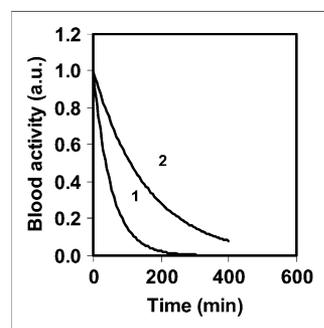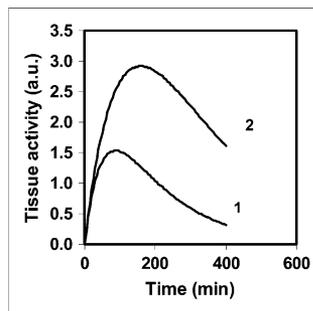
FIGURE 2. Theoretic ^{18}F-FDG tissue time–activity curve from Equation 4 for $T_{1/2} = 37$ min (1) and from Equation 5 for $T_{1/2} = 110$ min (2). Values of $\lambda C_p(t=0)$ and K have been arbitrarily set to 1 and 0.05 min^{-1}, respectively. a.u. = arbitrary unit.

similar to those found for $T_{1/2} = 110$ min in the 60- to 90-min range. The value of R for $T_{1/2} = 37$ min at $t = 45$ min is 2.7 times lower than that for $T_{1/2} = 110$ min at $t = 160$ min.

DISCUSSION

A 2-compartment model has allowed us to compare the time–activity curve of ^{18}F-FDG tissue uptake in patients who have normal renal function with that of a theoretic limiting case that leads to the highest possible patient radiation dose (for an arbitrary injected activity) and the longest possible time to peak tracer activity in tissues. The conditions of this limiting case have been arbitrarily set to define extremes for tracer activities to be injected and acquisition times. The condition of the highest possible patient radiation dose is achieved when one assumes that the plasma decay of the tracer is the tracer physical decay. The second condition is fulfilled with the first condition since the tracer plasma decay is the longest one possible, and the second condition also requires the tracer to be trapped irreversibly because the occurrence of a release rate constant can lessen the time to peak tracer activity (2). An anuric patient might fulfill the first condition but would not fulfill the second condition. Indeed, the anuric-patient radiation dose is the highest possible, even if some tracer is taken up in whole-body tissues; however, this last feature is not exactly compatible with the second condition of the proposed framework, that is, the longest possible time to peak tracer activity in tissues (even if the tracer may be partly released back to the blood). Furthermore, the model presented here assumes that, in patients with normal renal function, the ^{18}F-FDG blood time–activity curve monoexponentially decays after the injection, although it has been shown that the ^{18}F-FDG plasma clearance was triexponential (8). It is suggested that,

FIGURE 1. Theoretic ^{18}F-FDG blood time–activity curve for $T_{1/2} = 37$ min (patient with normal renal function) (1) and $T_{1/2} = 110$ min (limiting case) (2). Value of $\lambda C_p(t=0)$ has been arbitrarily set to 1. a.u. = arbitrary unit.
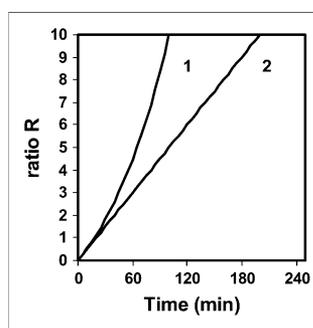
FIGURE 3. Ratio R vs. time delay between ^{18}F-FDG injection and PET acquisition for $T_{1/2} = 37$ min (patient with normal renal function) (1) and $T_{1/2} = 110$ min (limiting case) (2).

in a first approximation, the use of a monoexponential input function in this work may be justified: the third exponential function of a triexponential input function represents the major portion of the whole-blood ^{18}F-FDG available to the tumor, 89% by Hunter (8); the ^{18}F-FDG tissue time–activity curves using a tri- or monoexponential input function are similar; and this work emphasizes PET beyond 1 h after the tracer injection, when the third part of a triexponential input function plays the only role.

The comparison of the ^{18}F-FDG tissue time–activity curve in the limiting case with that of a patient who has normal renal function (Fig. 2) shows that the more severe the renal failure is, the longer is the blood tracer availability to the tissue, the greater is ^{18}F-FDG tissue uptake, and the later does tracer activity in the tissue maximize (with a limit of 160 min). This reasoning may be extended to the standardized uptake value (SUV) of a tissue, which includes trapped tracer, that is, $C_T(t)$ (Eqs. 4 and 5), and free tracer in the blood and interstitial volumes. Consequently, in patients with renal failure, the tissue SUV should be overestimated (when comparing 2 similar patients with and without renal failure and using similar PET examination parameters). As an example, although free tracer in the blood and interstitial volumes is not considered in the present model, Figure 2 shows that at 60 min after ^{18}F-FDG injection, the tissue SUV might be about 1.4 times greater in the limiting case than in a patient with normal renal function. However, the tissue SUV should be overestimated in patients with renal failure unless the failure indirectly impairs tissue sensitivity to insulin and hence glucose metabolism (10). Indeed, besides results in various tissues showing an SUV overestimation, Minamimoto et al. reported a small but significant decrease of ^{18}F-FDG accumulation in the brains of patients with suspected renal failure, compared with healthy volunteers (11). Although the relationship between kidney disease and insulin resistance of the brain is not known, these authors discussed this particular result with the results of other investigators studying diabetes (12,13).

This work presents 2 extremes, that is, normal renal function and a theoretic limiting case, whereas real patients present a spectrum of renal function between these 2 extremes. Therefore, in current clinical practice, this work leads us to propose landmark injected activities and acquisition times for the use of ^{18}F-FDG PET in patients with renal failure. To obtain a patient radiation dose and tissue ^{18}F-FDG uptake similar to those of patients without renal failure, and to reduce the dose to the medical staff, we suggest that the injected activity be lowered and that the static PET acquisition be obtained later, depending on the severity of renal failure: the more severe the failure, the lower the injected activity and the later the imaging. Although the model does not allow us to accurately propose what activity should be injected and what imaging timing should be used in a patient with arbitrary renal failure (i.e., between the 2 extremes of normal function and the theoretic limiting case), the model nevertheless suggests that it is not necessary to divide the usually injected activity by a factor of more than 3 or to start the imaging beyond t = 160 min after injection. Indeed, the study of the limiting case shows that to obtain a similar radiation dose to that of patients without renal failure, the injected activity should be divided by a factor of 3 and that one cannot fully compensate for such a lowering factor by performing the acquisition at t = 160 min, since the value of $C_T(t)$ for $T_{1/2}$ = 110 min is "only" 2.3 times greater than that at t = 45 min for patients with normal renal function (usual timing in current practice). However, the ratio R, reflecting the tumor-to-background ratio, for $T_{1/2}$ = 110 min at t = 160 min is 2.7 times greater than that for $T_{1/2}$ = 37 min at t = 45 min.

CONCLUSION

This work shows that ^{18}F-FDG PET in patients with renal failure can be achieved with an optimized radiation dose, without reducing the tracer tissue uptake: the more severe the renal failure, the lower the injected activity (without exceeding a factor of 3) and the later the imaging (without necessarily beginning the acquisition beyond 160 min after injection). Furthermore, the model also shows that the more severe the renal failure is, the more overestimated is the SUV, unless the renal failure indirectly impairs tissue sensitivity to insulin and hence glucose metabolism.

REFERENCES

1. Laffon E, Allard M, Marthan R, Ducassou D. A method to quantify the uptake rate of 2-[^{18}F]fluoro-2-deoxy-D-glucose in tissues. *Nucl Med Commun.* 2004;25: 851–854.
2. Laffon E, Allard M, Marthan R, Ducassou D. A method to quantify at late imaging a release rate of ^{18}F-FDG in tissues. *CR Biol.* 2005;328:767–772.
3. ICRP publication 53: radiation dose to patients from radiopharmaceuticals (addendum 5). In: *Annals of the ICRP.* Oxford, U.K.: Pergamon Press; 2001: 5–11.
4. Hays MT, Segall GM. A mathematical model for the distribution of fluorodeoxy-glucose in humans. *J Nucl Med.* 1998;40:1358–1366.
5. Hays MT, Watson EE, Thomas SR, Stabin M. MIRD dose estimate report no. 19: radiation absorbed dose estimates from ^{18}F-FDG. *J Nucl Med.* 2002;43: 210–214.
6. Delbeke D, Coleman RE, Guiberteau MJ, et al. Procedure guideline for tumor imaging with ^{18}F-FDG PET/CT. *J Nucl Med.* 2006;47:885–895.
7. Shiozaki T, Sadato N, Senda M, et al. Noninvasive estimation of FDG input function for quantification of cerebral metabolic rate of glucose: optimization and multicenter evaluation. *J Nucl Med.* 2000;41:1612–1618.
8. Hunter GJ, Hamberg LM, Alpert NM, Choi NC, Fischman AJ. Simplified measurement of deoxyglucose utilization rate. *J Nucl Med.* 1996;37:950–955.
9. Strauss LG, Dimitrakopoulou-Strauss A, Koczan D, et al. ^{18}F-FDG kinetics and gene expression in giant cell tumors. *J Nucl Med.* 2004;45:1528–1535.
10. DeFronzo RA, Alvestrand A, Smith D, Hendler R, Hendler E, Wahren J. Insulin resistance in uremia. *J Clin Invest.* 1981;67:563–568.
11. Minamimoto R, Takahashi N, Inoue T. FDG-PET of patients with suspected renal failure: standardized uptake values in normal tissues. *Ann Nucl Med.* 2007; 21:217–222.
12. Bingham EM, Hopkins D, Smith D, et al. The role of insulin in human brain glucose metabolism. *Diabetes.* 2002;51:3384–3390.
13. Hasselbalch SG, Knudsen GM, Videbaek C, et al. No effect of insulin on glucose blood-brain barrier transport and cerebral metabolism in humans. *Diabetes.* 1999; 48:1915–1921.